

See discussions, stats, and author profiles for this publication at: <https://www.researchgate.net/publication/228507432>

# Radiationless Deactivation Process of 1-Dimethylamino-9-fluorenone Induced by Conformational Relaxation in the Excited State: A New Model Molecule for the TICT Process

ARTICLE in THE JOURNAL OF PHYSICAL CHEMISTRY A · OCTOBER 2002

Impact Factor: 2.69 · DOI: 10.1021/jp0203604

CITATIONS

35

READS

47

8 AUTHORS, INCLUDING:



Akimitsu Morimoto

Mitsui Chemicals

4 PUBLICATIONS 121 CITATIONS

SEE PROFILE



László Biczók

Hungarian Academy of Sciences

110 PUBLICATIONS 2,574 CITATIONS

SEE PROFILE



Tomoyuki Yatsuhashi

Osaka City University

64 PUBLICATIONS 908 CITATIONS

SEE PROFILE



Donald A. Tryk

University of Yamanashi

249 PUBLICATIONS 15,474 CITATIONS

SEE PROFILE

# Radiationless Deactivation Process of 1-Dimethylamino-9-fluorenone Induced by Conformational Relaxation in the Excited State: A New Model Molecule for the TICT Process

Akimitsu Morimoto,<sup>†</sup> László Biczók,<sup>‡</sup> Tomoyuki Yatsuhashi,<sup>‡,§</sup> Tetsuya Shimada,<sup>†</sup> Shingo Baba,<sup>†</sup> Hiroshi Tachibana,<sup>†</sup> Donald A. Tryk,<sup>†</sup> and Haruo Inoue<sup>\*,†,||</sup>

Department of Applied Chemistry, Graduate Course of Engineering, Tokyo Metropolitan University, 1-1 Minami-ohsawa, Hachiohji, Tokyo 192-0397, Japan, Chemical Research Center, Hungarian Academy of Sciences, P.O. Box 17, 1525 Budapest, Hungary, and CREST (Japan Science and Technology)

Received: February 7, 2002; In Final Form: July 23, 2002

The deactivation process of excited 1-(dimethylamino)-9-fluorenone (1-DMAF) was investigated by means of steady-state and time-resolved fluorescence spectroscopy. Fluorescence decay profiles for 1-DMAF, which has a relatively short lifetime (several tens of picoseconds in low viscosity solvents at ambient temperature) are much affected by the fluidity of the surrounding solvent. The lifetimes increase in glassy solvents at 77 K as well as with increasing viscosity. These results indicate that conformational relaxation by the dimethylamino group plays an important role in the deactivation process of 1-DMAF. Detailed analysis of the temperature dependence of the fluorescence lifetime revealed that the conformational relaxation process has a very small intramolecular activation barrier (5.4 kJ/mol). Results of MO calculations suggest that the dimethylamino moiety of 1-DMAF is pretwisted in the ground state and that the most stable structure in the excited state is a twisted intramolecular charge transfer (TICT) state. 1-DMAF could be a new model molecule that exhibits the TICT phenomena.

## 1. Introduction

Electronic excited states of molecules having intramolecular charge transfer excited states are affected not only by solvent relaxation of the surrounding solvent but also by conformational relaxation of the excited molecule itself. Above all, it has been reported that the excited states of many aromatic dimethylamino compounds deactivate efficiently by conformational relaxation at the dimethylamino moiety.<sup>1–14</sup> One of the best-known typical examples is the twisted intramolecular charge transfer (TICT) process of dimethylaminobenzonitrile (DMABN),<sup>1–5</sup> proposed by Grabowski.<sup>1,2</sup>

The conformational relaxation of DMABN has been rationalized by the twisting motion of the dimethylamino group toward a perpendicular conformation, coupled with intramolecular electron transfer to the aromatic ring in order to minimize the orbital overlap between the cation at the dimethylamino moiety and anion at the aromatic moiety. Also, the intramolecular conformational relaxation process is complicated by the crossing of the potential energy curves for the first singlet excited state ( $S_1$ ) and second singlet excited state ( $S_2$ ) due to a difference of the degree of stabilization by the polar solvent.<sup>4,6,8–10</sup>

At present, several mechanisms other than TICT have been proposed in order to explain the conformational relaxation of DMABN.<sup>6–9</sup> Zaccariasse et al., for example, examined the fluorescence spectroscopy for many DMABN derivatives and reported that the mechanism of the conformational relaxation

is not a TICT process but a planar intramolecular charge transfer (PICT) process, in which the dimethylamino, which has  $sp^3$ -like structure, converts to a planar  $sp^2$  structure to achieve intramolecular charge transfer without twisting of the dimethylamino group.<sup>8</sup> Other mechanisms, for example, the WICT<sup>6a</sup> (wagged ICT) model, in which the dimethylamino group wags and in so doing forms a pyramidal structure in the excited state, and the RICT<sup>6b</sup> (rehybridization ICT) model, in which the cyano group undergoes a change in hybridization in the excited state, have also been proposed. To establish which mechanism is valid, theoretical calculations<sup>7</sup> and time-resolved vibrational spectroscopy<sup>11,12</sup> have been performed by several groups. Phillips et al., have carried out a time-resolved resonance Raman study of DMABN and its derivatives to distinguish between the TICT, PICT, WICT, and RICT mechanisms.<sup>11</sup> They successfully detected and identified the frequency of the phenyl-amino stretching mode and observed the downshift of the mode, a result that is well harmonized with the TICT mechanism. More examples are further required to understand the conformational relaxation phenomena in more detail, especially to establish whether the TICT model can be generally applied to other systems or not.

A step toward simplification and further understanding of the conformational relaxation process is to separate the first singlet excited state and upper excited singlet state to avoid the crossing and an interaction between the two excited states such as the proximity effect.<sup>13,14</sup> Molecules exhibiting strong intramolecular charge transfer (ICT) may be good probes, because the first absorption band of such molecules consists of the ICT excited-state only, and the energy of the ICT excited state ( $S_1$ ) is sufficiently separated from the second excited state ( $S_2$ ) to neglect the interaction between the two excited states ( $S_1$  and  $S_2$ ).

\* Corresponding author. E-mail: inoue-haruo@c.metro-u.ac.jp.

<sup>†</sup> Tokyo Metropolitan University.

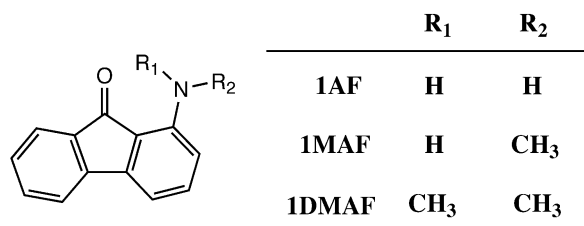
<sup>‡</sup> Hungarian Academy of Sciences.

<sup>§</sup> Present address: department of Chemistry, Faculty of Science, Osaka City University, 3–3–138 Sugimoto, Sumiyoshi, Osaka 558-8585, Japan.

<sup>||</sup> CREST (Japan Science and Technology).

**TABLE 1: Photophysical Properties of 1-Aminofluorenones at 298 K<sup>a</sup>**

compound	solvent	$\Phi_f$ (10 <sup>2</sup> )	$\tau_f$ (ns)	$E_{0-0}$ (10 <sup>4</sup> cm <sup>-1</sup> )	$k_f$ (10 <sup>7</sup> s <sup>-1</sup> )	$k_{ISC}$ (10 <sup>8</sup> s <sup>-1</sup> )	$k_{IC}$ (10 <sup>8</sup> s <sup>-1</sup> )
1-AF	acetonitrile	5.7	2.3	2.16	2.5	4.2	0.045
	EtOH	6.8	4.0	2.10	1.7	2.0	0.35
1-MAF	acetonitrile	6.5	4.2	2.04	1.7	2.1	1.1
	EtOH	6.4	2.8	2.01	2.3	2.0	1.4
1-DMAF	acetonitrile	0.05	0.02	2.02	2.0	0.0	440
	EtOH	0.05	0.02	2.01	2.2	0.0	480

<sup>a</sup> References 15 and 17.**Figure 1.** Molecular structures of the 1-aminofluorenones used in the present work.

For the past several years, we have been studying the photophysical properties of aminofluorenones having ICT excited states.<sup>15–17</sup> The deactivation process of aminofluorenones is strongly dependent on the type and substitution at the amino group. We have already found that excited 1-DMAF deactivates efficiently via internal conversion, unlike other 1-aminofluorenones [1-aminofluorenone (1-AF) and 1-methylaminofluorenone (1-MAF)], which deactivate mainly by intersystem crossing, as summarized in Table 1.<sup>15,17</sup>

Deviations from a linear correlation between the ionization potential of the electron-donating group and the absorption maximum and the results of simple MO calculations both suggest that the dimethylamino group of 1-DMAF suffers steric hindrance from the carbonyl oxygen, and a conformational relaxation process may play an important role in the deactivation process of excited 1-DMAF.<sup>15,17</sup> In this paper, we have extended our investigation to confirm and discuss the conformational relaxation process by means of steady-state and time-resolved fluorescence measurements and observation of their temperature and viscosity effects.

## 2. Experimental Section

The structures of the 1-aminofluorenones used in this paper are shown in Figure 1. The preparation and purification of these compounds were reported previously.<sup>13</sup> All solvents employed were spectrometric grade.

The absorption spectra were recorded on a Shimadzu UV-2100PC spectrophotometer, and the corrected fluorescence spectra were measured with a Hitachi F-4010 spectrofluorometer. The time-resolved fluorescence spectra were measured with a polychromator (CHROMEX 250IS)-streakscope (Hamamatsu, C4334) system. The samples were excited by 450-nm light pulse from an optical parametric generator (EKSPLA, PV-401, 420–650 nm, fwhm 25 ps, > 1 mJ) pumped by a third harmonic of Nd:YAG laser (EKSPLA, PL2143B, 25 ps fwhm, 15 mJ, 5 Hz), under time-correlated single photon counting conditions. The laser flux was adjusted by attenuation with neutral density filters to avoid multiphoton absorption processes and nonlinear effects. The control of solvent temperature was carried out with a cryostat (Oxford, ITC601). Fluorescence decay profiles after the time region of solvent relaxation (~10 ps) were almost same among all wavelengths monitored. Consequently, the decay profiles of all conditions were fitted by single-exponential

function in all wavelength regions (480–650 nm). The deuterium isotope effect on the fluorescence decay in ethanol was measured with a femtosecond fluorescence up-conversion system (CDP systems, FOG-100). The fundamental of a Ti:sapphire laser (800 nm, 1 kHz<sub>r</sub>) was used to generate the second harmonic (400 nm) in a BBO nonlinear crystal. The second harmonic was used for excitation of the sample, and the remaining fundamental was delayed and used as a probe beam to up-convert the fluorescence signal in the BBO nonlinear crystal. The up-converted signal, after passing through a monochromator, was detected with a photomultiplier. The fwhm of the instrumental response, estimated by cross-correlation, was 200 fs. The sample cell (thickness = 1 mm) was rotated to avoid any heating effect. The concentration of 1-DMAF was 1.0 × 10<sup>-4</sup> M for all time-resolved emission measurements.

The microscopic viscosities of the solvents at various temperatures were measured by the fluorescence depolarization method using perylene as a probe molecule. The procedure has been described elsewhere.<sup>18</sup>

Molecular orbital (MO) calculations were performed with MOPAC 97 (PM3, C. I. = 6). The details of the optimization procedure will be described in section 3.3.

## 3. Results and Discussion

**3.1. Confirmation of Conformational Relaxation.** *3.1.1. Rigid Solvent Effect.* Solute motions such as rotation are strongly inhibited in a glassy solvent.<sup>21</sup> Supposing that there is some conformational relaxation process, photophysical properties should be much affected in a glassy solvent. From this point of view, fluorescence spectra and the resulting lifetime of 1-DMAF were measured in ethanol at 77 K and compared with those at 298 K. These results are shown in Figure 2 and Table 2. At 77 K, the fluorescence intensity was strengthened and the decay lifetime was much greater than that at 298 K. Such behavior was not observed for 1-AF and 1-MAF (Table 2). The fluorescence spectrum at 77 K showed a slight blue shift as compared with that at 298 K. This shift is presumably caused by a restriction of solvent relaxation in the solvent glass. Furthermore, we could observe phosphorescence in methyltetrahydrofuran (MTHF) at 77 K, while the triplet yield measured at ambient temperature was negligible (Table 1). These results strongly suggest that there is a deactivation pathway that involves a change of molecular conformation and is much more efficient than radiative decay or intersystem crossing at ambient temperature. The conformational change is inhibited at 77 K to suppress the nonradiative decay and increase the relative contribution of a radiative process or intersystem crossing to the triplet excited state.

We have reported that the molecules having an ICT excited state deactivate efficiently through hydrogen bonding.<sup>15–17,23,24</sup> Therefore, one may consider also that excited 1-DMAF in ethanol deactivates partly via intermolecular hydrogen bonding. Our recent study, however, reported that the degree of ICT

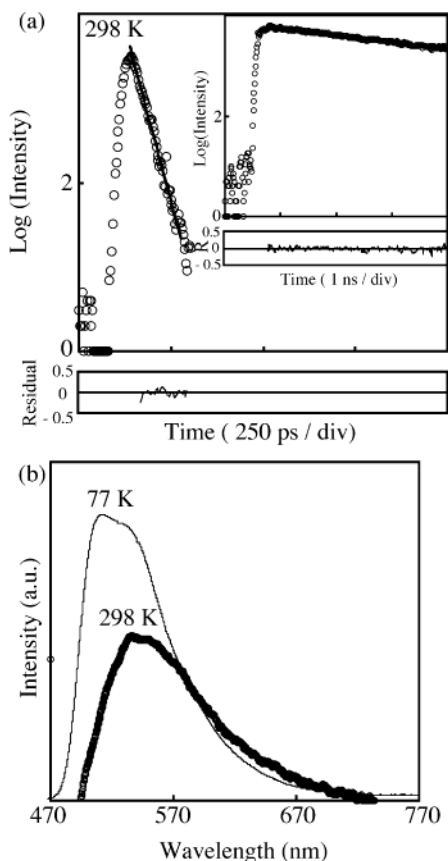


**Figure 2.** Fluorescence decay profile (a) and spectra (b) of 1-DMAF in ethanol at 298 and 77 K. Excitation wavelength was 450 nm. Analyzed emission wavelength was 480–650 nm. [1-DMAF] =  $1.0 \times 10^{-4}$  M.

**TABLE 2: Fluorescence Lifetimes of 1-Aminofluorenones at 77 and 298 K (RT)**

compound	lifetime in ethanol (ns)	
	298 K	77 K
1-AF	4.0	2.7
1-MAF	2.8	3.5
1-DMAF	0.02	2.8
1-DMAF(in MTHF) <sup>a</sup>	0.03	2.8

<sup>a</sup> In methyltetrahydrofuran.

estimated for 1-aminofluorenones is not so large compared to that for the other aminofluorenones, and thus the deactivation rate is not greatly affected by hydrogen bonding.<sup>17</sup> Moreover, we observed almost no deuterium isotope effects on the fluorescence decay of 1-DMAF in ethanol-O-H and ethanol-O-D (Figure 3). This result clearly indicates that deactivation induced by hydrogen bonding does not affect the excited 1-DMAF at all.

**3.1.2. Solvent Viscosity Effects.** If the deactivation process of 1-DMAF is governed by some motion of a certain atomic group, the motion should also be influenced by the solvent viscosity. To verify the existence of conformational relaxation, the solvent viscosity dependence on the fluorescence lifetime was examined at 298 K. As described later, the photophysical properties of 1-DMAF are also affected by solvent polarity. To exclude the effect of solvent polarity, ethylene glycol and glycerin, which have different viscosities ( $\eta$  at 298 K: 18.9 cP for ethylene glycol and 566 cP for glycerin), and similar polarity (dielectric constant at 298 K: 37.7 for ethylene glycol and 42.5 for glycerin) and their mixtures were used for the measurements. The viscosity of each mixture was estimated by the fluorescence

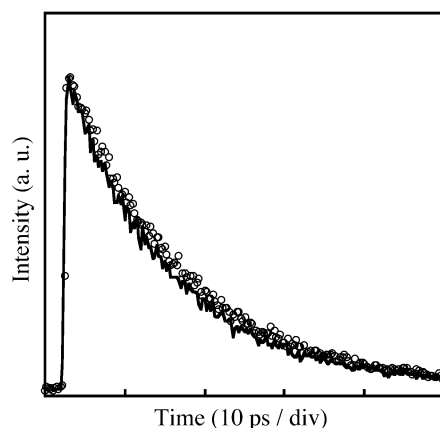


**Figure 3.** Deuterium isotope effects on the fluorescence decay of 1-DMAF in ethanol: (dotted profile) in ethanol; (lined profile) in deuterated ethanol (EtOD). Excitation wavelength was 450 nm. Analyzed emission wavelength was 650 nm. [1-DMAF] =  $1.0 \times 10^{-4}$  M.

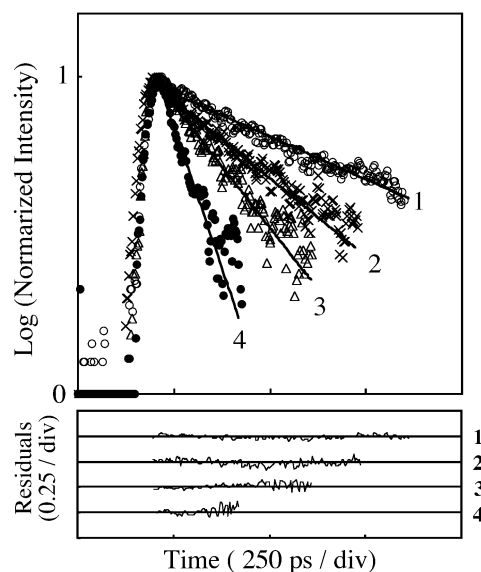


**Figure 4.** Fluorescence decay profiles of 1-DMAF at ambient temperature in glycerin, ethylene glycol, and their mixtures: (1) glycerin ( $\eta = 566$  cP); (2) glycerin/ethylene glycol = 4:1 ( $\eta = 168$  cP); (3) glycerin/ethylene glycol = 2:3 ( $\eta = 50.0$  cP); (4) ethylene glycol ( $\eta = 18.9$  cP). Excitation wavelength was 450 nm. Analyzed emission wavelength was 480–650 nm. [1-DMAF] =  $1.0 \times 10^{-4}$  M.

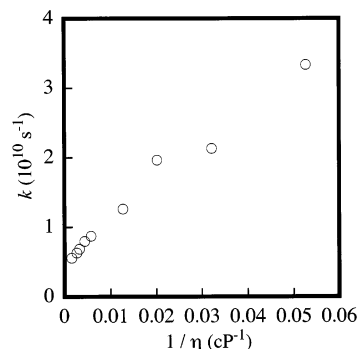


**Figure 5.** Correlation between deactivation rate of 1-DMAF ( $k$ ) and the reciprocal of the viscosity ( $1/\eta$ ).

depolarization of perylene. The results are shown in Figures 4 and 5. All of the decay profiles were fitted by single-exponential functions. The fluorescence lifetimes showed an increase with increasing viscosity. All of the results thus indicate that the

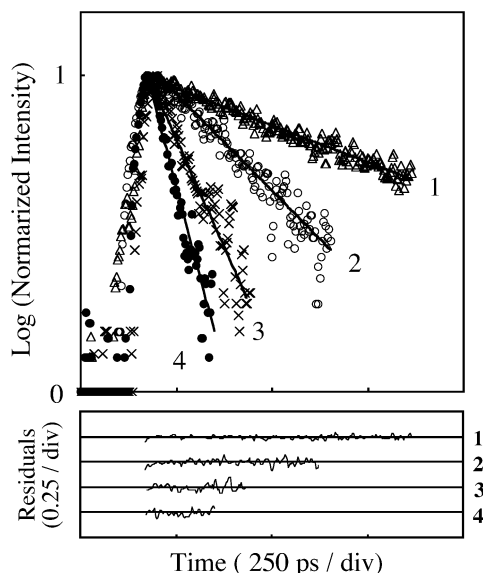


**Figure 6.** Fluorescence decay profiles of 1-DMAF in ethanol at 160 K (1), 190 K (2), 230 K (3), and 260 K (4). Excitation wavelength was 450 nm. Analyzed emission wavelength was 480–650 nm. [1-DMAF] =  $1.0 \times 10^{-4}$  M.

efficient deactivation of the excited 1-DMAF is induced by conformational relaxation of the molecule. This result clearly indicates that the deactivation of 1-DMAF is strongly governed by solvent viscosity. Judging from the molecular rigidity of the fluorenone skeleton, the motion of the dimethylamino group must be responsible for the conformational relaxation.

### 3.2. Activation Energy for Conformational Relaxation.

#### 3.2.1. Temperature Dependence on Fluorescence Lifetime.

Figure 6 presents fluorescence decay profile changes of 1-DMAF in the temperature range 165–298 K in ethanol. From this figure, it can be seen that a temperature decrease leads to an increase of fluorescence lifetime. On the other hand, the absorption spectra did not show particular changes other than a slight red shift ( $\sim 4$  nm) due to solvent polarity change and absorbance change with the change of solvent expansion in this temperature range (165–298 K). The decay profiles could be fitted by single-exponential functions, and the time constants obtained by the fitting can be regarded as conformational relaxation times, because the 1-DMAF lifetime is almost completely governed by the conformational relaxation, and the other deactivation rates (radiative decay and intersystem crossing) are small enough to neglect compared to the conformational relaxation time [see section 3.1 and Table 1: even the shortest decay at 165 K ( $k = 3.8 \times 10^9 \text{ s}^{-1}$ ) as shown in Figure 6 is much faster than the radiative decay ( $k_f = 3.8 \times 10^9 \text{ s}^{-1}$ )]. In this case, the deactivation rate can be closely correlated with the diffusional motion of the solute represented as a diffusion-controlled process. Supposing that the diffusion process follows Stokes–Einstein behavior (eq 1), the deactivation rate should be proportional to the temperature and inversely proportional to the viscosity.

$$k = \frac{AT}{\eta} \quad (1)$$

Here,  $k$ ,  $\eta$ ,  $T$ , and  $A$  are the deactivation rate constant of 1-DMAF, the solvent viscosity, the solvent temperature, and a constant, respectively. However, the plots of deactivation rate constant vs temperature divided by viscosity ( $T/\eta$ ) did not show a linear relationship (Figure 7). The deviation from eq 1 suggests

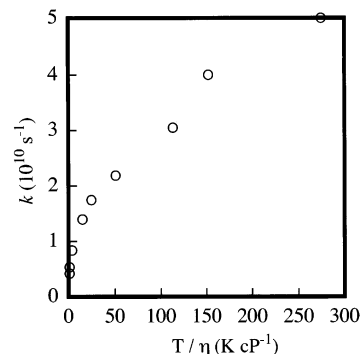


**Figure 7.** Correlation between the deactivation rate of 1-DMAF ( $k$ ) and the temperature divided by the solvent viscosity ( $T/\eta$ ).

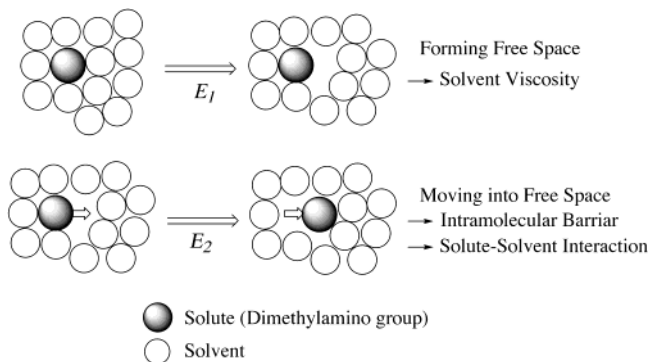


**Figure 8.** Diffusion process proposed for a microviscosity model that includes two processes (making free space and moving into the free space; see ref 22).

that a more microscopic interpretation should be applied to obtain a more correct description of the conformational relaxation process. Therefore, the decay rate constant was analyzed by taking the free volume concept into consideration.

**3.2.2. Concept of the Free Volume.** The treatment of the free volume in the diffusion process is reviewed by Birks et al.<sup>22</sup> in detail. In this paper, we give only the essence.

When microscopic and macroscopic friction are taken into consideration, the rotational and translational diffusion process should include two processes: (a) a process by which the surrounding solvent makes free volume, and (b) a process by which the dimethylamino group moves into the free space created by the surrounding solvent molecules (Figure 8). The former process should strongly depend on solvent viscosity, and the latter process should be dependent on the interaction between solvent and solute (dimethylamino group) and the intramolecular activation barrier. In this case, the deactivation rate of 1-DMAF, which is equal to the rotational diffusion rate of the dimethylamino group, is expressed by eq 2:

$$\frac{k\eta}{T} = A + B \exp(E_1 - E_2)/RT \quad (2)$$

Here,  $E_1$ , and  $E_2$  are the activation energies for each process in Figure 7 and  $R$  is the gas constant.  $E_1$  in eq 2 corresponds to the activation energy of the viscosity and can be obtained easily by use of an Arrhenius-type equation (eq 3).

$$\eta = \eta' \exp(E_1/RT) \quad (3)$$

Here,  $\eta'$  is the viscosity at infinite temperature. To obtain the activation energy of viscosity ( $E_1$ ) in ethanol, the viscosity was estimated by the fluorescence depolarization method<sup>18</sup> by use of perylene as a probe. An Arrhenius-type plot for solvent



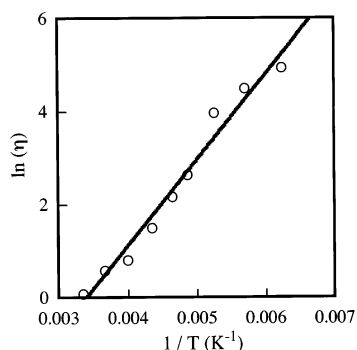


Figure 9. Arrhenius type plot for the viscosity of ethanol.

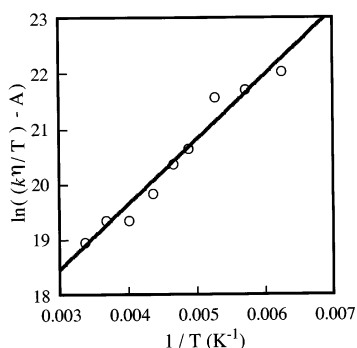


Figure 10. Arrhenius-type plot for the conformational relaxation of 1-DMAF taking the microdiffusion process into consideration.

viscosity obtained by the fluorescence depolarization method is shown in Figure 9. The logarithm of viscosity showed good linearity with the reciprocal of temperature. This indicates that the depolarization process of perylene is not affected by the latter process, in which the perylene moves into free space and is determined only by viscous flow of the surrounding solvent. The activation energy obtained by the slope in Figure 9 (15.5 kJ/mol) thus can be employed as the activation energy of viscosity.

**3.2.3. Evaluation of Intramolecular Activation Energy.** According to eq 2, the logarithm of  $k\eta/T - A$  was plotted vs the reciprocal of temperature by choosing the value  $A$ . The results are shown in Figure 10. The good linearity of the plots with the value of  $A = 1.1 \times 10^7$  (cP/K·s) supports the validity of eq 2. Substituting  $E_1$  estimated from eq 3 into eq 2, we obtain an  $E_2$  value of 5.4 kJ/mol from the slope. As mentioned above (section 3.2.2), the activation energy  $E_2$  is independent of solvent viscosity and dependent on the intramolecular barrier and the interaction between the dimethylamino group and the solvent (ethanol). It is expected that the interaction between the dimethylamino group and ethanol should be small, because most of such an interaction is nonspecific and thus weak. A possible specific interaction, e.g., hydrogen bonding between the lone pair of the dimethylamino nitrogen and the alcohol proton, becomes rather small by intramolecular charge transfer transition from the dimethylamino nitrogen to the carbonyl oxygen. Therefore, 5.4 kJ/mol of  $E_2$  should correspond mainly to the intramolecular activation barrier for conformational relaxation, and the results obtained from eqs 2 and 3, and Figures 9 and 10 suggest that the intramolecular activation energy of 1-DMAF for conformational relaxation is rather small. Such a fast deactivation process dependent on solvent viscosity is similar to that reported for the molecular propeller triphenylmethane dyes.<sup>27,28</sup> The mechanism of ultrafast decay of the triphenylmethanes has been well explained in terms of a barrierless potential.<sup>28</sup>

TABLE 3: Solvent Decay Rate Constant and Solvent Properties (298 K)

solvent	$\eta$ (cP) <sup>a</sup>	$\epsilon$ <sup>b</sup>	$k$ (10 <sup>10</sup> s <sup>-1</sup> ) <sup>c</sup>
benzene	0.60	2.27	3.2
butyronitrile	0.60	24.8	4.0
ethanol	1.08	24.6	4.8
1-octanol	7.36	10.3	1.7
1,4-butandiol	71.5	30.2	1.5
ethylene glycol	18.9	37.7	3.4

<sup>a</sup> Solvent viscosity (ref 19). <sup>b</sup> Dielectric constant (ref 19). <sup>c</sup> Deactivation rate constant (reciprocal of fluorescence lifetime).

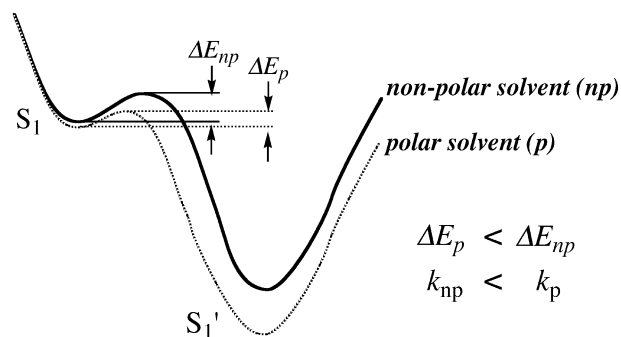
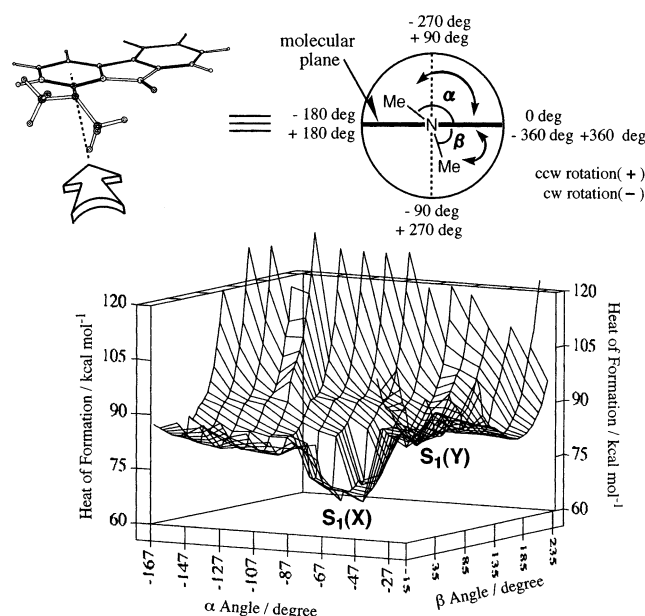


Figure 11. Potential curve of the conformational relaxation process of 1-DMAF excited in polar and nonpolar solvents.  $\Delta E_p$  and  $\Delta E_{np}$  are the activation energy for conformational relaxation in the polar and nonpolar solvents, respectively.  $k_p$  and  $k_{np}$  denote deactivation rate in polar and nonpolar solvents, respectively.

**3.3. The Properties and Structure after Conformational Relaxation.** **3.3.1. Solvent Polarity and Hydrogen Bonding Effects.** The property of the state after conformational relaxation can be discussed in terms of a solvent polarity effect on the fluorescence decay rate. The decay rates of 1-DMAF in several solvents are shown in Table 3. From Table 3, it can be seen that the decay rate was affected not only by solvent viscosity but also by solvent polarity and hydrogen bonding ability (see the results in benzene, butyronitrile, and ethanol). This result suggests that as compared with benzene, increasing solvent polarity (butyronitrile) and hydrogen bonding (ethanol) lead to a decrease in the activation energy for conformational relaxation. This behavior is explained based on the interpretation that the state after conformational relaxation is stabilized by a polar solvent, and hydrogen bonding at the carbonyl oxygen<sup>15</sup> and the degree of the stabilization is greater than that of the initial ICT excited state (Figure 11). Based on the speculation that the state after conformational relaxation should have a larger dipole moment than the initial ICT excited state, the relaxed state is probably an intramolecular charge-separated (ICS) state, where the intramolecular charge transfer from the nitrogen atom to the carbonyl oxygen is more distinct and complete charge separation is established by the rotation of the dimethylamino group.

In this study, emission of the state after conformational relaxation could not be observed. To explain this result, the following hypotheses were considered: (1) the energy of the conformational relaxation state is so stabilized that radiationless deactivation is promoted according to the energy-gap law;<sup>24</sup> (2) radiative decay is forbidden by the collapse of the symmetry of 1-DMAF after conformational relaxation at the dimethylamino group; and (3) the potential energy curve of  $S_1$  crosses that of  $S_0$ , and a nonadiabatic transition from the conical intersection may occur.<sup>25</sup> To evaluate these hypotheses, transient absorption studies and ultrafast spectroscopic studies are now in progress.



**Figure 12.** Definition of dihedral angle ( $\alpha$ ,  $\beta$ ) and correlation between heat of formation and dihedral angle ( $\beta$ ) at each fixed  $\alpha$  (see in text).  $S_1(X)$  is the minimum giving the lowest heat of formation, and  $S_1(Y)$  is the nearest local minimum to the ground state (Franck–Condon state). The abbreviations cw and ccw indicate clockwise and counterclockwise, respectively.

**3.3.2. Estimation of the Most Stable Structure after Conformational Relaxation by MO Calculation.** As shown above, the existence of an ICS state generated by conformational relaxation was proposed on the basis of the experimental results. To estimate how the dimethylamino group changes conformation and what the conformation of the ICS state is, semiempirical (PM3) MO calculations were performed for the ground ( $S_0$ ) and excited states ( $S_1$ ). The conformational change of the dimethylamino group was represented by changes in the two dihedral angles between the two methyl groups attached to the nitrogen and the fluorenone ring ( $\alpha$  and  $\beta$  in Figure 12). The  $\alpha$  values were fixed at 15 discrete positions (every 10 degrees between  $-27^\circ$  and  $-167^\circ$ ), and the heat of formation was evaluated by structural optimization without any constraints except the fixed values of  $\alpha$  and  $\beta$ . The angle  $\beta$  was varied gradually with respect to each value of  $\alpha$  (Figure 12). At the pair of  $\alpha$  and  $\beta$  values giving the minimum heat of formation, optimization was performed again without any constraint, and the structure obtained was then considered to be the most stable structure for the ground ( $S_0$ ) and excited states [ $S_1(X)$  in Figure 12]. In the ground state, the most stable conformation was revealed to be at  $\alpha = -80^\circ$  and  $\beta = 149^\circ$ , namely, the dimethylamino group is pretwisted with respect to the fluorenone plane. For the excited  $S_1$  state, the MO calculation afforded very interesting and suggestive information about the conformational relaxation. Two local minimum points [ $S_1(Y)$  and  $S_1(X)$ ] were distinctly observed, as shown in Figure 12. The  $S_1(Y)$  state, which is the nearest local minimum to the ground state, has almost the same conformation of dimethylamino group, with  $\alpha = -77^\circ$  and  $\beta = 151^\circ$ , with that of the ground state. The state  $S_1(Y)$ , thus, should be nearly the Franck–Condon excited state. Another local minimum point  $S_1(X)$ , which is more stabilized than  $S_1(Y)$ , has an almost perpendicular conformation of the dimethylamino group with respect to the fluorenone plane ( $\alpha = -87^\circ$  and  $\beta = 87^\circ$ ). Since the state  $S_1(Y)$  is situated on a shallow minimum potential surface, the excited 1-DMAF would be expected to slide down easily to the more stable minimum point, ( $S_1(X)$ ), where the dimethylamino group is completely twisted

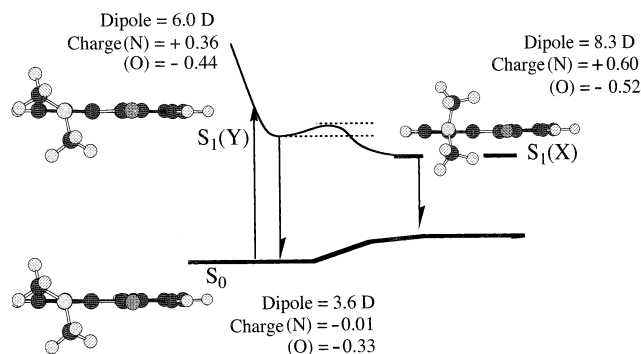


**Figure 13.** Optimized structure of 1-DMAF estimated by MO calculations in the ground and excited state.

in perpendicular direction with respect to the fluorenone plane. To estimate an activation energy for the conformational relaxation from  $S_1(Y)$  to  $S_1(X)$ , the potential energy change was estimated for a reaction pathway of a straightforward conversion from  $S_1(Y)$  to  $S_1(X)$  on the potential surface of the excited state indicated in Figure 12. Figure 13 shows the reaction pathway. Excitation of the pretwisted ground state to the excited Franck–Condon state leads to the  $S_1(Y)$  state in a shallow local minimum that allows the further relaxation to the more stable state  $S_1(X)$  with an activation energy of 2.0 kJ/mol, which is comparable to the experimentally obtained value of 5.4 kJ/mol. Substantial increases in the dipole moment and the negative charge on the carbonyl oxygen and the positive charge on the dimethylamino nitrogen in the twisted structure [ $S_1(X)$ ] indicate that the twisting of the dimethylamino group is coupled with the intramolecular electron transfer. Figure 13 clearly shows that the structure of the ICS state after conformational relaxation is a TICT state.

Recently, an interesting rotational relaxation behavior of 1-dimethylaminonaphthalene has been reported, where a pretwisted dimethylamino group in the Franck–Condon state reverts to a planar position to induce an efficient deactivation.<sup>13,14</sup> The deactivation induced by the rotational relaxation was explained in relation to the potential energy surface-crossing. The rotation in this case is in the reverse direction to that for the TICT phenomena. The compound used in the present work, 1-DMAF, however, exhibits a rotation to a completely twisted form, with a more highly charge-transferred (charge-separated) state as described above. 1-DMAF, thus, provides a well-defined model for understanding the TICT phenomena.

Aminofluorenones include a large number of derivatives and thus studies of other fluorenones, having various substituents at various positions (e.g., 4-dimethylaminofluorenone and 4-pyrrolylfluorenone) and the comparison of their behavior with that of 1-DMAF, will provide sufficient information and explanation for the mechanism of conformational relaxation. Aminofluorenones could be good probe molecules for understanding TICT phenomena.

**Acknowledgment.** This work was partly supported by a Grant-in Aid from the Ministry of Education, Science, Sports, and Culture of Japan.

## References and Notes

- (1) Grabowski, Z.; Dobkowski, J. *Pure Appl. Chem.* **1983**, 245.
- (2) Rotkiewicz, K.; Grelmann, K. H.; Grabowski, Z. *R. Chem. Phys. Lett.* **1973**, 19, 315.
- (3) Rettig, W.; Lippert, E. *J. Mol. Struct.* **1980**, 61, 17.
- (4) Rettig, W. *Angew. Chem., Int. Ed. Engl.* **1986**, 25, 971.
- (5) Rotkiewicz, K.; Rubszewska, W. *Chem. Phys. Lett.* **1980**, 70, 444.

- (6) (a) Schuddeboom, W.; Jonker, S. A.; Warman, J. M.; Leinhos, U.; Kühnle, W.; Zachariasse, K. A. *J. Phys. Chem.* **1992**, *96*, 10809. (b) Sobolewski, A. L.; Domcke, W.; *Chem. Phys. Lett.* **1996**, *259*, 119.
- (7) (a) Gorse, A.; Pesquer, M.; *J. Phys. Chem.* **1995**, *99*, 4039. (b) Sudholt, W.; Sobolewski, A. L.; Domcke, W.; *Chem. Phys.* **1999**, *240*, 9. Sobolewski, A. L.; Sudholt, W.; Domcke, W.; *J. Phys. Chem. A* **1998**, *102*, 2716. Parusel, A. B. J.; Kohler, G.; Grimme, S. *J. Phys. Chem. A* **1998**, *102*, 6297.
- (8) Zachariasse, K. A.; Grobys, M.; von der Haar, Th.; Hebecker, A.; Il'ichev, Yu. V.; Ziang, Y.-B.; Morawski, O.; Kuhnle, W. *J. Photochem. Photobiol. A: Chem.* **1996**, *102*, 59. Zachariasse, K. A.; Grobys, M.; von der Haar, Th.; Hebecker, A.; Il'ichev, Yu. V.; Morawski, O.; Ruckert, I.; Kuhnle, W. *J. Photochem. Photobiol. A: Chem.* **1997**, *105*, 373.
- (9) Rettig, W.; Bliss, B.; Dirnberger, K. *Chem. Phys. Lett.* **1999**, *305*, 8. Okada, T.; Uesugi, M.; Kohler, G.; Rechthaler, K.; Rotkiewicz, K.; Rettig, W.; Grabner, G. *Chem. Phys.* **1999**, *241*, 327.
- (10) Zachariasse, K. A. *Chem. Phys. Lett.* **2000**, *320*, 8.
- (11) (a) Kwok, W. M.; Ma, C.; Phillips, D.; Matousek, P.; Parker, A. W.; Towrie, M. *J. Phys. Chem. A* **2000**, *104*, 4188. Ma, C.; Kwok, W. M.; Matousek, P.; Parker, A. W.; Phillips, D.; Toner, W. T.; Towrie, M. *J. Photochem. Photobiol. A: Chem.* **2001**, *142*, 177. Ma, C.; Kwok, W. M.; Matousek, P.; Parker, A. W.; Phillips, D.; Toner, W. T.; Towrie, M. *J. Phys. Chem. A* **2001**, *105*, 4648. (b) Kwok, W. M.; Ma, C.; Matousek, P.; Parker, A. W.; Phillips, D.; Toner, W. T.; Towrie, M.; Umapathy, S. *J. Phys. Chem. A* **2001**, *105*, 984.
- (12) Chudoba, C.; Kummrow, A.; Dreyer, J.; Stenger, J.; Nibbering, E. T. J.; Elsaesser, T.; Zachariasse, K. A. *Chem. Phys. Lett.* **1999**, *309*, 357.
- (13) Rückert, I.; Demeter, A.; Morawski, O.; Kühnle, W.; Tauer, E.; Zachariasse, K. A. *J. Phys. Chem. A* **1999**, *103*, 1958.
- (14) Suzuki, K.; Tanabe, H.; Tobita, S.; Shizuka, H. *J. Phys. Chem. A* **1997**, *101*, 4496. Suzuki, K.; Demeter, A.; Kuhnle, W.; Tauer, E.; Zachariasse, K. A.; Tobita, S.; Shizuka, H. *Phys. Chem. Chem. Phys.* **2000**, *2*, 981.
- (15) Yatsuhashi, T.; Nakajima, Y.; Shimada, T.; Inoue, H. *J. Phys. Chem. A* **1998**, *102*, 3018.
- (16) Yatsuhashi, T.; Nakajima, Y.; Shimada, T.; Inoue, H. *J. Phys. Chem. A* **1998**, *102*, 8657.
- (17) Biczók, L.; Yatsuhashi, T.; Bérces, T.; Inoue, H. *Phys. Chem. Chem. Phys.* **2001**, *3*(6), 980.
- (18) Shinitzky, M.; Dianoux, A. C.; Gitler, C.; Weber, G. *Biochemistry* **1971**, *10*(11), 2106.
- (19) Riddick, J. A.; Bunger, W. B.; Sakano, T. K. in *Organic Solvents*, Vol. 2, Wiley: New York, 1986.
- (20) Reynald, L.; Gardecki, J. A.; Frankland, J. V.; Horng, M. L.; Maroncelli, M. *J. Phys. Chem.* **1996**, *100*, 10337. Horng, M. L.; Gardecki, J. A.; Maroncelli, M. *J. Phys. Chem. A* **1997**, *101*, 1030.
- (21) Horng, M. L.; Gardecki, J. A.; Papazyran, A.; Maroncelli, M. *J. Phys. Chem.* **1995**, *99*, 17311.
- (22) Alwattar, A. H.; Lumb, M. D.; Birks, J. B. in *Organic Molecular Photophysics*, Vol. 1, Birks, J. B. Ed., Wiley: New York, 1973, Chapter 8.
- (23) Gierer, A.; Wirtz, K. *Z. Naturforsch.* **1953**, *8a*, 532.
- (24) Inoue, H.; Hida, M.; Nakashima, N.; Yoshihara, K. *J. Phys. Chem.* **1982**, *86*, 3184. Yatsuhashi, T.; Inoue, H. *J. Phys. Chem.* **1997**, *101*, 8166. Morimoto, A.; Yatsuhashi, T.; Shimada, T.; Kumazaki, S.; Yoshihara, K.; Inoue, H. *J. Phys. Chem. A* **2001**, *105*, 8840.
- (25) Morimoto, A.; Yatsuhashi, T.; Shimada, T.; Biczók, L.; Tryk, D. A.; Inoue, H. *J. Phys. Chem. A* **2001**, *105*, 10488.
- (26) Michl, J.; Klessinger, M. *Excited States and Photochemistry of Organic Molecules*, VCH: New York, 1995.
- (27) Baba, S.; Tachibana, H.; Inoue, H. to be submitted.
- (28) Vogel, M.; Rettig, W. *Ber. Bunsen-Ges. Phys. Chem.* **1985**, *89*, 962. Cremers, D. A.; Windsor, M. W. *Chem. Phys. Lett.* **1980**, *71*, 27.
- (29) Ben-Amotz, D.; Harris, C. B. *J. Chem. Phys.* **1987**, *86*(9), 4856. Ben-Amotz, D.; Jeanloz, R.; Harris, C. B. *J. Chem. Phys.* **1987**, *86*(11), 6119.